Sakata model of hadrons revisited. II. Nuclei and scattering

Eugene V. Stefanovich
1763 Braddock Court, San Jose, CA 95125, USA
eugene_stefanovich@usa.net

January 14, 2017

Abstract

This article continues our previous study in arXiv:1010.0458. Sakaton interactions potentials are re-optimized. Masses of mesons, baryons, light nuclei and hypernuclei are obtained in a fair agreement with experiment. Total elastic scattering cross sections (pp, $p\bar{p}$, np, and Λp) are also close to experimental data in a broad range of momenta 0.1 - 1000 GeV/c. Our results suggest that Sakata model could be a promising alternative to the quark model of hadrons.

1 Introduction

Quark model is universally accepted as the foundation of the modern theory of strong nuclear interactions and the entire Standard Model. However, in spite of numerous successes, the idea of quarks is susceptible to criticism. For example, the postulated quarks and gluons cannot be directly observed, even in principle. These particles are assumed to possess very unusual properties, such as fractional electric charges and non-observable color. The mechanism of quark confinement inside mesons and baryons has not been understood yet. QCD calculations of quark bound states [1] or low-energy scattering processes are notoriously difficult.

So, one is tempted to ask provocative questions: is the nature of strong interactions bound to be so complicated? are there alternative ways to think about the physics of hadrons? One such alternative idea was proposed by S. Sakata in 1956 [2], i.e., long before the advent of the quark model. The beauty of the Sakata model was that the number of arbitrary assumptions was reduced to a minimum. Elementary constituents (sakatons) were chosen to be the familiar proton (p), neutron (n), and

Lambda-hyperon (Λ).[1] In analogy with electrostatic interactions between charges, it was assumed that sakaton-sakaton and antisakaton-antisakaton interaction potentials are strongly repulsive, but sakaton-antisakaton potentials are equally attractive, thus leading to unusually high defects of mass, especially in pure sakaton-antisakaton meson states. It was satisfying that, unlike in the quark model, the nature of the sakaton binding in elementary particles was similar to the usual pattern observed in molecular and nuclear physics, where the mass of a compound system is lower than the sum of masses of its constituents. The interaction between sakatons drops to zero when they are pulled apart to large distances, so that readily observable constituents are recovered.

1.1 Matumoto's mass formula

The above ideas about sakaton binding were summarized in a simple mass formula proposed by K. Matumoto [4, 5]. In this formula, the mass of a multisakaton system was calculated as the sum of masses of the constituents[2] plus the sum of interaction energies (divided by c^2) for all sakaton pairs. These interaction energies were simply defined as constants[3]

$$\begin{aligned} E(\nu,\nu) &= E(\overline{\nu},\overline{\nu}) = -E(\nu,\overline{\nu}) = 1740MeV \\ E(\nu,\Lambda) &= E(\overline{\nu},\overline{\Lambda}) = -E(\nu,\overline{\Lambda}) = -E(\overline{\nu},\Lambda) = 1561MeV \\ E(\Lambda,\Lambda) &= E(\overline{\Lambda},\overline{\Lambda}) = -E(\Lambda,\overline{\Lambda}) = 1275MeV \end{aligned}$$

Table 1: Model properties of sakatons.

sakaton symbol	Mass MeV/c^2	Electric charge	Strangeness	Spin
n	940	0	0	1/2
p	940	1	0	1/2
Λ	1116	0	-1	1/2

For example, in the Sakata model the Σ^- baryon is identified with a bound state of two sakatons and one antisakaton $\Sigma^- = \Lambda n\overline{p}$. Then by Matumoto's formula one immediately obtains its mass

[1] In this work we consider only systems possessing up, down, and strange flavors. By adding the fourth elementary hadron Λ_c^+, one can extend the Sakata model to charmed particles as well [3].

[2] See Table 1.

[3] Here we use symbol ν to collectively denote nucleons n and p.

$$
\begin{aligned}
m(\Sigma^-) &= m(\Lambda n\overline{p}) = m(\Lambda) + m(n) + m(p) + E(\Lambda, n)/c^2 + E(\Lambda, \overline{p})/c^2 + E(n, \overline{p})/c^2 \\
&= (1116 + 940 + 940 + 1561 - 1561 - 1740)\ MeV/c^2 = 1256\ MeV/c^2
\end{aligned}
$$

which is not far from the experimental value of 1189 MeV/c^2. This simple estimate should be contrasted with the enormous complexity of *ab initio* QCD calculations [1], which are impossible without powerful supercomputers.

1.2 Sakatons vs. quarks

In Table 2 we collected predictions of the Matumoto's mass formula for some hadrons. This formula is doing a pretty good job for common mesons (π, K) and baryons (Σ, Ξ). It even predicts the instability of Δ resonances,[4] which are not distinguished from stable baryons in the quark model.

Table 2: Comparison of the Sakata and quark models

Particle	Sakaton composition	Mass from Matumoto's formula, MeV/c^2	Exp. mass MeV/c^2	Quark composition
π^-	$n\overline{p}$	140	**140**	$d\overline{u}$
K^-	$\Lambda\overline{p}$	495	**494**	$s\overline{u}$
Δ^-	$nn\overline{p}$	unstable	unstable	ddd
Σ^-	$\Lambda n\overline{p}$	1256	**1189**	dds
Ξ^-	$\Lambda\Lambda\overline{p}$	1325	**1322**	dss
Ω^-	$\Lambda\Lambda\Lambda\overline{pn}$	1427	**1672**	sss
Ω^{--}	$\Lambda\Lambda\Lambda\overline{pp}$	1427	not seen	not predicted
Ω^0	$\Lambda\Lambda\Lambda\overline{nn}$	1427	not seen	not predicted
??	$\Lambda\Lambda\overline{pp}$	883	not seen	not predicted

In the Sakata-Matumoto approach, the famous Ω^- baryon is stable with respect to all possible channels of dissociation, even though this particle is a bound state of five sakatons. However, at this point the luck of the model ends, as it incorrectly predicts stability of the two other members (Ω^{--} and Ω^0) of the isospin triplet. Similarly, the model predicts non-existent tetrasakatons, like $\Lambda\Lambda\overline{pp}$. Such predictions could be taken seriously in the beginning of 1960's when not all members of the particle zoo were known. However, in 2017 we can be sure that such exotic particles do not exist. Should this failure be sufficient for disqualifying the Sakata model?

[4]The predicted mass of $\Delta^-(= nn\overline{p})$ is 1080 MeV/c^2, which corresponds to zero energy of dissociation into n and $\pi^- = n\overline{p}$.

We think that such a conclusion would be premature, because the primitive Matumoto mass formula cannot be reliable. In our previous publication [3] we designed a set of inter-sakaton potentials and calculated masses of multisakaton bound states by numerical solution of the corresponding Schrödinger equations. A good agreement was obtained with the mass spectrum and stabilities of known mesons and baryons. However, there were also two areas, in which our previous results appeared inadequate:

1. When attempting to model particle collisions, we found that scattering cross sections of hadrons were overestimated by several orders of magnitude.

2. Our *pn*, *pp* and *nn* potentials were completely repulsive, so they could not explain the binding of protons and neutrons in nuclei.

In this work we decided to recalibrate sakaton interaction potentials for better description of these two important aspects.

2 Theory and computational details

2.1 Model Hamiltonian

In our opinion, it should be possible to build a theory of strong interactions based on the idea of point particles interacting by instantaneous forces. This belief is supported by the success of the "dressed particle" approach to relativistic quantum field theories [6, 7, 8, 9], where fields are replaced by directly interacting particles, while all scattering properties and bound state energies are preserved and the renormalization is not needed.

Thus we chose to describe an interacting $\mathcal{N}$-sakaton system by the approximate non-relativistic Hamiltonian

$$H = \sum_{i=1}^{\mathcal{N}} m_i c^2 + \sum_{i=1}^{\mathcal{N}} \frac{p_i^2}{2m_i} + \sum_{i<j}^{\mathcal{N}} V_{ij}(r_{ij}) \tag{1}$$

where $\mathbf{p}_i, r_{ij} \equiv |\mathbf{r}_i - \mathbf{r}_j|$ are momenta of the sakatons and their relative distances, respectively. Masses m_i of sakatons are shown in Table 1.

To proceed with calculations, we have to specify sakaton-sakaton interaction potentials $V(r)$ in (1). Despite identification of sakatons with real particles p, n, Λ^0, this information is not readily available. Indeed, many accurate nucleon-nucleon potentials were reported in the literature [10, 11, 12, 13, 9], but much less is known about nucleon-antinucleon, nucleon-Λ^0, and $\Lambda^0 - \Lambda^0$ interactions. Moreover, existing potentials are usually fitted to reproduce low-energy properties, like binding energies of nuclei (few

MeV) and scattering amplitudes for collision energies below 1 GeV. However, in order to represent deep sakaton binding in mesons and baryons, we need potentials that describe strong attraction ($E < -1.5$ GeV) in sakaton-antisakaton pairs and equally strong repulsion ($E > 1.5$ GeV) in sakaton-sakaton pairs at short distances. Unfortunately, existing studies were not interested in these distance/energy ranges.

So, we decided to optimize our own distance-dependent functions $V(r)$, which were chosen as superpositions of three Yukawa potentials

$$V_{ij}(r) = A_{ij} z_i z_j \frac{e^{-\alpha_{ij} r}}{r} + B_{ij} \frac{e^{-\beta_{ij} r}}{r} + C_{ij} z_i z_j \frac{e^{-\gamma_{ij} r}}{r} \tag{2}$$

where $z_i = +1$ for sakatons and $z_i = -1$ for antisakatons. Optimized parameters of these potentials are collected in Table 3. Interaction (2) consists of three parts. The first term is of the Matumoto type. It corresponds to the attraction in sakaton-antisakaton pairs ($z_i z_j = -1$) and equal repulsion in sakaton-sakaton and antisakaton-antisakaton pairs ($z_i z_j = 1$). Our preliminary tests indicated that this interaction alone was inadequate as it systematically overestimated binding and thus predicted stability of many nonexistent species. Some extra repulsion was provided by the second term. The third term was designed to represent the long-range ($r > 0.6\ fm$) nucleon-nucleon attraction responsible for the binding in nuclei.

Table 3: Parameters of sakaton-sakaton interaction potentials (2) optimized in this work.

	A MeV·fm	α fm^{-1}	B MeV·fm	β fm^{-1}	C MeV·fm	γ fm^{-1}
$p-p$	2137	8.2	1119	10.04	-12	0.125
$n-n$	2137	8.2	1119	10.04	-12	0.125
$p-n$	1610	7.02	886.6	14.55	-18.6	0.106
$p-\Lambda$	1334	7.245	386.8	10.726	-21	0.25
$n-\Lambda$	1334	7.245	386.8	10.726	-21	0.25
$\Lambda-\Lambda$	709	9.13	500	11.15	-22	0.30

As an example, in Fig. 1 we show the proton-proton interaction potential $V_{pp}(r)$ by a thick full line. The proton-neutron potential $V_{pn}(r)$ (thin full line) has a similar shape, but the attractive well at $r \approx 1\ fm$ is somewhat deeper, so that a bound state of the deuteron (pn) can be supported (see Table 6). These functions are comparable to well-known models of nucleon-nucleon interactions: the Malfliet-Tjon potential [14] and the scalar portion of the Reid potential [10], though in our case the attractive well is somewhat shallower and wider. The proton-antiproton interaction $V_{p\overline{p}}(r)$ (broken line) is almost a mirror image of the pp potential. Other sakaton-antisakaton potentials have

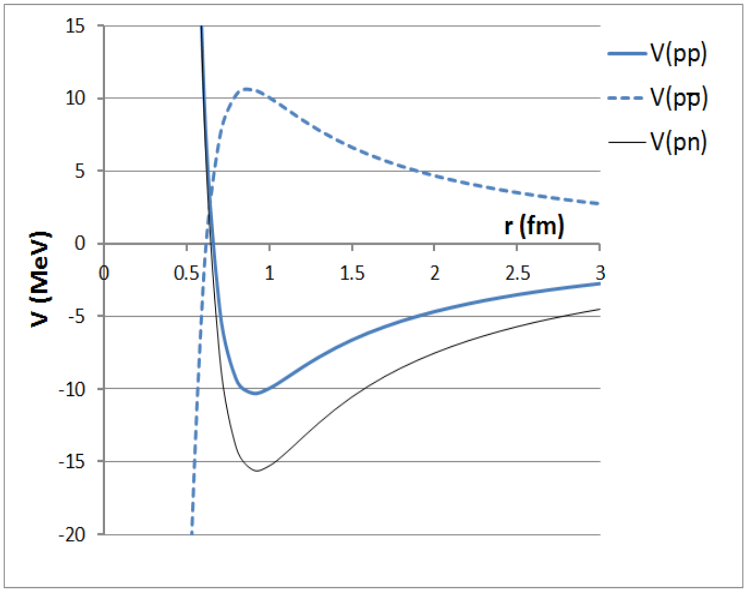

Figure 1: Interaction potentials: proton-proton (thick full line), proton-neutron (thin full line), and proton-antiproton (broken line).

similar shapes. Their deep attractive wells at $r < 0.6\ fm$ are responsible for holding sakatons inside mesons and baryons.

Note that in our approximation p and n sakatons have equal masses and the same interaction parameters. This implies that all properties calculated here (masses and scattering cross-sections) are invariant with respect to simultaneous sakaton replacements $p \leftrightarrow n$.

2.2 Bound state calculations

Bound state energies of multisakaton systems were calculated using the stochastic variational method of Varga and Suzuki [15, 16]. The FBS computer program [17] was downloaded from the CPC Program Library (Queen's University of Belfast, N. Ireland). Only ground states with the lowest total spin ($s = 0$ for bosons and $s = 1/2$ for fermions) and zero orbital momentum were considered here. The basis set size depended on the number of sakatons in the system. For mixed sakaton-antisakaton species with particle numbers $\mathcal{N} = 2,\ 3,\ 4,\ 5$ the basis size was $K = 50,\ 220,\ 250,$ and 800, respectively. For sakaton-only species (i.e., nuclei and hypernuclei) the basis size $K = 50$ was independent on the number of particles. For other computational parameters explained in [17] we used values $M_0 = 10, K_0 = 50, b_{min} = 10^{-6}$, and $b_{max} = 10$. They were adjusted for optimal balance between the accuracy and the speed of convergence.

2.3 Scattering calculations

Scattering calculations were performed in the first Born approximation [18, 19].[5] For the differential cross section of two particles colliding with momenta $\mathbf{p}_1 = -\mathbf{p}_2 \equiv \mathbf{p}_{c.m}$ in the center-of-mass frame we used formula[6]

$$\frac{d\sigma}{d\Omega} = \frac{(2\pi)^4\hbar^2|T_B(\mathbf{k})|^2}{c^4}\left(\frac{1}{E_1(p_{c.m.})}+\frac{1}{E_2(p_{c.m.})}\right)^{-2} \tag{3}$$

where $E_i(p) \equiv \sqrt{m_i^2c^4+p^2c^2}$ are energies of the colliding particles, $\mathbf{k} \equiv \mathbf{p}_1' - \mathbf{p}_1$ is the transferred momentum and matrix element T_B is the Fourier transform of the interaction potential (2)

$$\begin{aligned} T_B(\mathbf{k}) &= \frac{1}{(2\pi\hbar)^3}\int d\mathbf{r}e^{\frac{i}{\hbar}\mathbf{kr}}V(\mathbf{r}) \\ &= \frac{1}{2\pi^2\hbar}\left(\frac{A_{ij}z_iz_j}{\hbar^2\alpha_{ij}^2+k^2}+\frac{B_{ij}}{\hbar^2\beta_{ij}^2+k^2}+\frac{C_{ij}z_iz_j}{\hbar^2\gamma_{ij}^2+k^2}\right) \end{aligned} \tag{4}$$

For comparison with experiments it is convenient to rewrite $d\sigma/d\Omega$ as a function of invariant Mandelstam variables[7] $s \equiv (\tilde{p}_1+\tilde{p}_2)^2$ and $t \equiv (\tilde{p}_1-\tilde{p}_1')^2$, which have simple meanings in the center of mass frame

$$\begin{aligned} s &= (E_1(p_{c.m.})+E_2(p_{c.m.}))^2 \\ t &= -c^2k^2 = 2c^2p_{c.m.}^2(\cos\theta-1) \end{aligned} \tag{5}$$

where θ is the scattering angle (between vectors $\mathbf{p}_1'$ and $\mathbf{p}_1$). Taking into account (5) and $d\Omega = 2\pi\sin\theta d\theta = -2\pi d(\cos\theta)$, we obtain the differential cross section as a function of $-t$ for two colliding protons ($m_1 = m_2 = m_p$) and high collision energies ($\sqrt{s} \gg m_pc^2$)

$$\begin{aligned} \frac{d\sigma}{dt} &= \frac{d\sigma}{d\Omega}\cdot\frac{2\pi}{dt/d(\cos\theta)} = \frac{d\sigma}{d\Omega}\cdot\frac{\pi}{c^2p_{c.m.}^2} \\ &= \frac{4\pi}{s-4m_p^2c^4}\cdot\frac{(2\pi)^4\hbar^2s}{16c^4}|T_B(\mathbf{k})|^2 \\ &\approx \pi\left(\frac{A_{pp}}{c^2\hbar^2\alpha_{pp}^2-t}+\frac{B_{pp}}{c^2\hbar^2\beta_{pp}^2-t}+\frac{C_{pp}}{c^2\hbar^2\gamma_{pp}^2-t}\right)^2 \end{aligned} \tag{6}$$

[5] This approximation is justified as we are interested primarily in the high energy scattering.

[6] see equation (3.149) in [19]

[7] Here we used tilde to denote energy-momentum 4-vectors $\tilde{p}_i$

The total elastic cross section was calculated by integrating the differential cross section (3) on angles

$$\sigma_{elastic}(p_{c.m.}) \;=\; 2\pi \int_0^{\pi} \sin\theta d\theta \frac{d\sigma}{d\Omega} \tag{7}$$

For easier comparison with experiments we switched to the laboratory reference frame[8] and expressed $\sigma_{elastic}$ as a function of the "lab frame" momentum of the incoming particle [9]

$$p_{lab} = p_{c.m.}\sqrt{s}/(mc^2)$$

So, in the case of equal masses, the lab frame cross section was obtained by replacing $p_{c.m.}^2 \to (mc\sqrt{m^2c^2 + p_{lab}^2} - m^2c^2)/2$ in formula (7).

3 Results

3.1 Bound states of sakatons

According to the Sakata model, all mesons and baryons, except p, n, and Λ^0, are in fact composite systems built from elementary sakatons and antisakatons. Atomic nuclei can be also regarded as multisakaton bound states. So, the first challenge for our model was to analyze the stability pattern of simplest compound systems listed in Table 4.[10]

As shown in Table 5, masses of light stable mesons and baryons are reproduced reasonably well in our model. In agreement with experiment, no stable tetrasakaton mesons were found and the only stable pentasakaton baryon is the observed $\Omega^- = \Lambda\Lambda\Lambda\overline{pn}$ particle.

As we mentioned in subsection 2.1, our potentials (2) were designed to describe nucleon-nucleon binding in atomic nuclei. Indeed, results presented in Table 6 demonstrate that the nuclear stability pattern is represented fairly well up to the ^{6}Be nucleus. However, the nuclear binding energies are systematically lower than the observed ones, which indicates that pp, pn, and nn attractions are underestimated in our model.[11]

[8] where the "target" particle 2 is at rest

[9] see eq. (46.36) in [20]

[10] We are interested only in the stability with respect to strong interactions. Particles experiencing weak and/or electromagnetic decays are regarded as stable here.

[11] For some species shown in Tables 6 and 7, our calculations did not converge, probably due to numerical instability of the FORTRAN code.

Table 4: Summary table of compound hadrons considered in this work. Notation: $\sigma = (p, n, \Lambda)$ stands for all sakatons; $\nu = (p, n)$ stands for nucleons.

Sakaton composition	Particle type	Comments	see Table
$\sigma\overline{\sigma}$	simple mesons	all stable except $\Lambda\overline{\Lambda}$	5
$\sigma\sigma\overline{\sigma}\overline{\sigma}$	tetrasakaton mesons	all unstable	
$\sigma\sigma\overline{\sigma}$	simple baryons	all unstable except Σ and Ξ	5
$\sigma\sigma\sigma\overline{\sigma}\overline{\sigma}$	pentasakaton baryons	all unstable except Ω^-	5
$\nu\nu\ldots\nu$	nuclei		6
$\nu\Lambda, \Lambda\Lambda, \nu\nu\Lambda, \nu\Lambda\Lambda$	hypernuclei		7

Table 5: Stable compound mesons and baryons. Masses, binding energies and preferable dissociation channels.

Stable particle	Sakaton composition	Calc. mass MeV/c^2	Exp. mass MeV/c^2	Calc. Binding energy (MeV)	Exp. Binding energy (MeV)
π^0	$(p\overline{p}, n\overline{n})$	323.99	**135**	$1556.01(\rightarrow p+\overline{p})$	$\mathbf{1733}(\rightarrow p+\overline{n})$
π^+	$p\overline{n}$	338.21	**140**	$1541.79(\rightarrow p+\overline{n})$	$\mathbf{1734}(\rightarrow p+\overline{n})$
π^-	$n\overline{p}$	338.21	**140**	$1541.79(\rightarrow n+\overline{p})$	$\mathbf{1734}(\rightarrow n+\overline{p})$
K^0	$\Lambda\overline{n}$	499.46	**498**	$1556.54(\rightarrow \Lambda+\overline{n})$	$\mathbf{1558}(\rightarrow \Lambda+\overline{n})$
K^-	$\Lambda\overline{p}$	499.46	**494**	$1556.54(\rightarrow \Lambda+\overline{p})$	$\mathbf{1556}(\rightarrow \Lambda+\overline{p})$
Σ^0	$(\Lambda p\overline{p}, \Lambda n\overline{n})$	1428.13	**1193**	$11.33(\rightarrow p+\Lambda\overline{p})$	$\mathbf{58}(\rightarrow \Lambda+p\overline{p})$
Σ^+	$\Lambda p\overline{n}$	1400.47	**1189**	$38.99(\rightarrow p+\Lambda\overline{n})$	$\mathbf{67}(\rightarrow \Lambda+p\overline{n})$
Σ^-	$\Lambda n\overline{p}$	1400.47	**1189**	$38.99(\rightarrow n+\Lambda\overline{p})$	$\mathbf{67}(\rightarrow \Lambda+n\overline{p})$
Ξ^0	$\Lambda\Lambda\overline{n}$	1231.32	**1315**	$388.14\ (\rightarrow \Lambda+\Lambda\overline{n})$	$\mathbf{299}(\rightarrow \Lambda+\Lambda\overline{n})$
Ξ^-	$\Lambda\Lambda\overline{p}$	1231.32	**1322**	$388.14\ (\rightarrow \Lambda+\Lambda\overline{p})$	$\mathbf{288}\ (\rightarrow \Lambda+\Lambda\overline{p})$
Ω^-	$\Lambda\Lambda\Lambda\overline{p}\overline{n}$	1720.95	**1672**	$9.83(\rightarrow \Lambda\Lambda\overline{n}+\Lambda\overline{p})$	$\mathbf{137}(\rightarrow \Lambda\Lambda\overline{n}+\Lambda\overline{p})$

In Table 7 we show binding energies for hypernuclei.[12] Our model correctly predicts the absence of $p\Lambda$, $n\Lambda$, and $\Lambda\Lambda$ bound states. However, the binding energy of the ${}^{3}_{\Lambda}H$ species is underestimated, and the model predicts positive binding of several non-existent species. This suggests that interaction parameters in Table 3 are not well balanced.

3.2 Elastic scattering

Calculated total elastic cross sections $\sigma_{elastic}(p_{lab})$ for pp, $p\overline{p}$, np, and Λp collisions are shown in Figs. 2, 3, 4, and 5, respectively. In these graphs we also showed results

[12] i.e., nuclei where one or more neutrons are replaced by Λ^0 particles

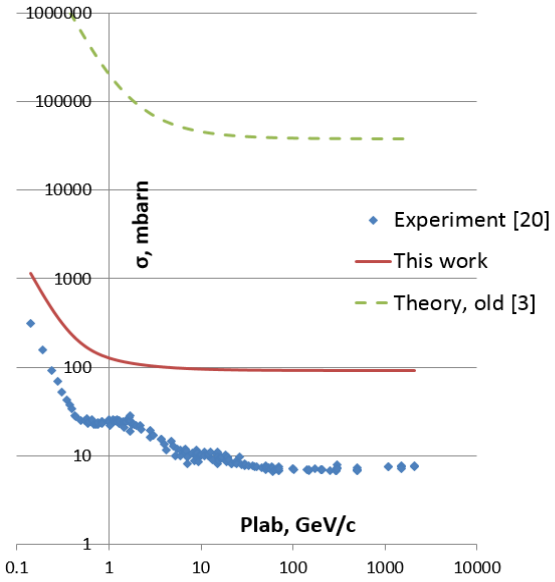

Figure 2: Total elastic cross sections for pp collisions.

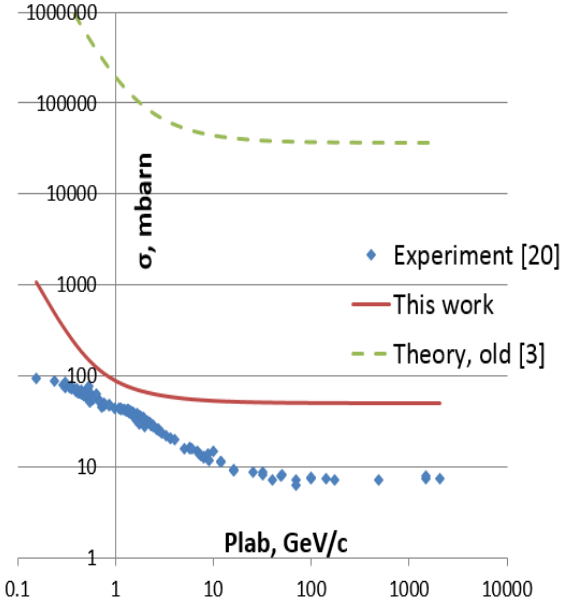

Figure 3: Total elastic cross sections for $p\overline{p}$ collisions.

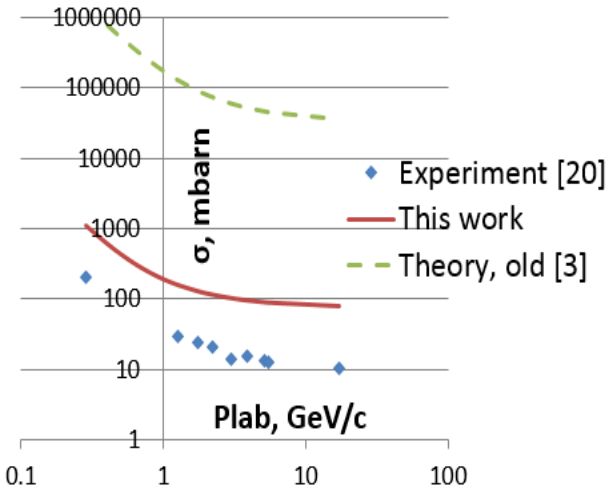

Figure 4: Total elastic cross sections for np collisions.

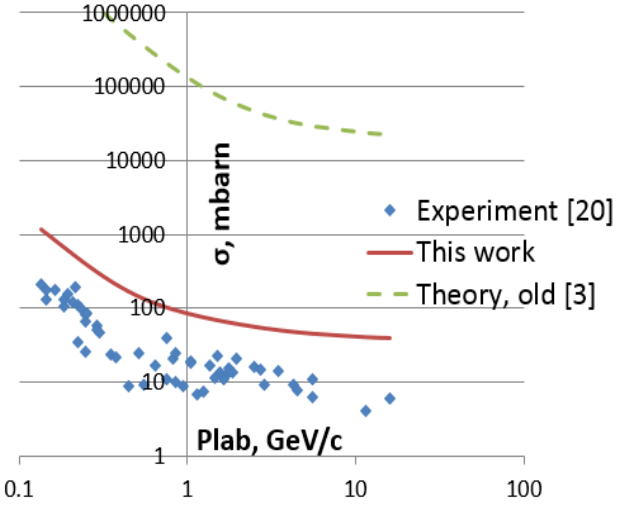

Figure 5: Total elastic cross sections for Λp collisions.

Table 6: Binding energies (with respect to complete dissociation) of light nuclei.

Sakaton composition	Nuclear symbol	Exp. binding energy (MeV) [21]	Calc. binding energy (MeV)
pp		0	0
pn	^{2}H	**2.22**	0.44
nn		0	0
ppp		0	diverged
ppn	^{3}He	**7.72**	1.75
pnn	^{3}H	**8.48**	1.75
nnn		0	diverged
pppp		0	0
pppn	^{4}Li	**4.62**	1.10
ppnn	^{4}He	**28.30**	1.08
pnnn	^{4}H	**5.50**	1.10
nnnn		0	0
ppppp		0	diverged
pppnn		0	0
ppnnn	^{5}Li	**26.33**	5.23
pnnnn	^{5}He	**27.41**	5.23
nnnnn	^{5}H	**1.08**	0
pppppp		0	diverged
ppppnn		0	0
pppnnn	^{6}Be	**26.92**	9.10
ppnnnn	^{6}Li	**31.99**	10.84
pnnnnn	^{6}He	**29.27**	9.10
nnnnnn	^{6}H	**5.78**	0
		0	0

obtained with sakaton potentials from our earlier work [3]. Our new potentials are more realistic, even though no special efforts were made to fit the experimental data [20]. We believe that the remaining discrepancy (of about one order of magnitude) can be removed by going beyond the first Born approximation in scattering calculations and further adjusting interaction potentials, in particular, adding spin-dependent terms there.

Table 7: Binding energies (with respect to complete dissociation) of hypernuclei.

Sakaton composition	Nuclear symbol	Exp. Binding energy (MeV) [22]	Calc. Binding energy (MeV)
$p\Lambda$		not seen	0
$n\Lambda$		not seen	0
$\Lambda\Lambda$		not seen	0
$pp\Lambda$		not seen	0.52
$pn\Lambda$	${}^{3}_{\Lambda}H$	**2.35**	1.30
$nn\Lambda$		not seen	0.52
$p\Lambda\Lambda$		not seen	0.72
$n\Lambda\Lambda$		not seen	0.72
$\Lambda\Lambda\Lambda$		not seen	diverged

4 Discussion and conclusions

The qualitative momentum dependence of our calculated total elastic scattering cross sections (see Figs. 2 - 5) was consistent with observations. However, the absolute values were overestimated by an order of magnitude. To understand this behavior, we turned to differential cross sections for pp collisions at $\sqrt{s} = 19.4\ GeV$ shown in Fig. 6. In our approximation (6), $d\sigma/dt$ does not depend on the collision energy $\sqrt{s}$. This property holds fairly well in experiments [23, 24, 25, 26].

The most significant deviation occurs at high values of the transferred momentum $(-t)$, where our calculated differential cross sections appear overestimated. Moreover, according to (6), the asymptotic decrease $d\sigma/dt \propto (-t)^{-2}$ is much slower than the observed one [23, 24, 25, 26]. This may explain the systematic overestimation of the total elastic cross sections in Fig. 2.

It is interesting to note that in our model the characteristic dip on the $d\sigma/dt$ curve occurs at $-t \approx 0.01\ GeV^2$, i.e. the value at which the parenthesis in (6) turns to zero. The cancellation of the three terms there becomes possible because the potential $V_{pp}(r)$ has both repulsive ($A_{pp} > 0, B_{pp} > 0$) and attractive ($C_{pp} < 0$) parts.

In spite of some deviations, meson, baryon, nuclear and hypernuclear stability patterns (Tables 5 - 7) are reproduced quite well in our studies. The most remarkable result is that our simple model predicts positive binding energies for all existing mesons and baryons, while dozens of exotic $\sigma\sigma\overline{\sigma}\overline{\sigma}$ and $\sigma\sigma\sigma\overline{\sigma}\overline{\sigma}$ species turn out to be unstable in agreement with observations. This is a strong indication that the Sakata model with simple interaction potentials does capture some important aspects of the physics of hadrons.

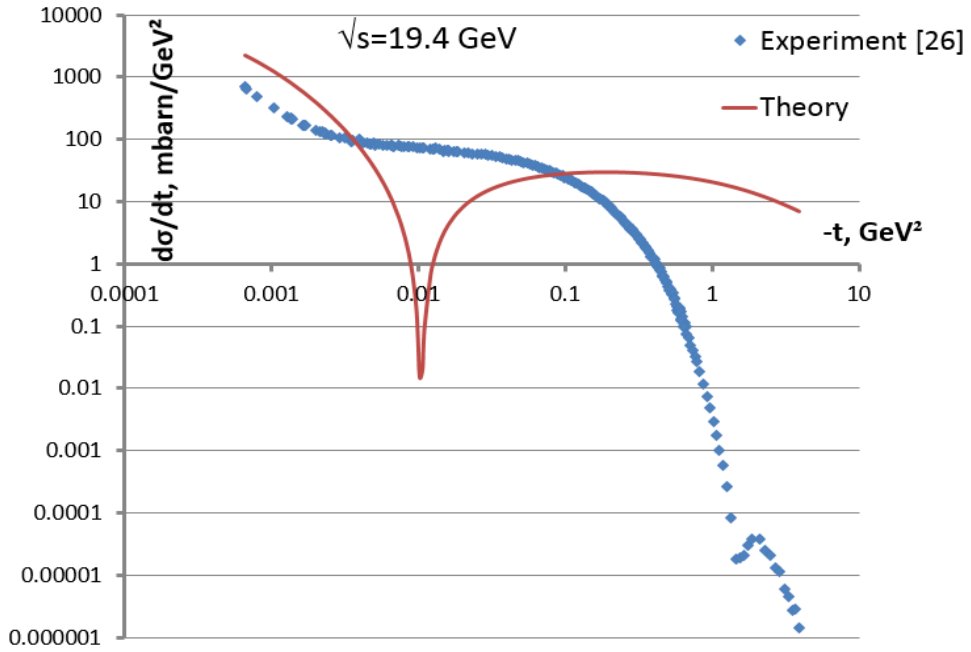

Figure 6: Differential cross section $d\sigma/dt$ for elastic pp collisions at $\sqrt{s} = 19.4$ GeV.

The author is grateful to Dr. A. V. Shebeko for enlightening discussions, critical comments, and continuing support.

References

[1] S.Durr and Z. Fodor and J. Frison and C. Hoelbling and R. Hoffmann and S.D. Katz and S. Krieg and T. Kurth and L. Lellouch and T. Lippert and K.K. Szabo and G. Vulvert, "Ab-initio determination of light hadron masses," *Science*, vol. **322**, p. 1224, 2008. arXiv:0906.3599v1.

[2] S. Sakata, "On a composite model for the new particles," *Prog. Theor. Phys.*, vol. **16**, p. 686, 1956.

[3] E. V. Stefanovich, "Sakata model of hadrons revisited," 2010. arXiv:1010.0458v1.

[4] K. Matumoto, "Some consequences of the compound hypothesis for elementary particles," *Prog. Theor. Phys.*, vol. **16**, p. 583, 1956.

[5] K. Matumoto, S. Sawada, Y. Sumi, and M. Yonezawa, "Mass formula in the Sakata model," *Prog. Theor. Phys. Suppl.*, vol. **19**, p. 66, 1961.

[6] E. V. Stefanovich, "Relativistic quantum dynamics," 2005. arXiv:physics/0504062v17.

[7] E. Stefanovich, *Relativistic Quantum Theory of Particles. II.* Saarbrücken: Lambert Academic Publishing, 2015.

[8] A. V. Shebeko and M. I. Shirokov, "Unitary transformations in quantum field theory and bound states," *Phys. Part. Nucl.*, vol. **32**, p. 15, 2001. arXiv:nucl-th/0102037v1.

[9] I. Dubovyk and O. Shebeko, "The method of unitary clothing transformations in the theory of nucleon–nucleon scattering," *Few-Body Systems*, vol. **48**, p. 109, 2010.

[10] G. E. Brown and A. D. Jackson, *The nucleon-nucleon interaction.* North-Holland, 1976.

[11] W. G. Love and M. A. Franey, "Effective nucleon-nucleon interaction for scattering at intermediate energies," *Phys. Rev. C*, vol. **24**, p. 1073, 1981.

[12] W. G. Love and M. A. Franey, "Nucleon-nucleon t-matrix interaction for scattering at intermediate energies," *Phys. Rev. C*, vol. **31**, p. 488, 1985.

[13] R. Machleidt, K. Holinde, and C. Elster, "The Bonn meson-exchange model for nucleon-nucleon interaction," *Phys. Rep.*, vol. **149**, p. 1, 1987.

[14] R. A. Malfliet and J. A. Tjon, "Solution of the Faddeev equations for the triton problem using local two-particle interactions," *Nucl. Phys. A*, vol. **127**, p. 161, 1969.

[15] K. Varga and Y. Suzuki, "Precise solution of few-body problems with the stochastic variational method on a correlated Gaussian basis," *Phys. Rev. C*, vol. **52**, p. 2885, 1995.

[16] Y. Suzuki and K. Varga, *Stochastic variational approach to quantum-mechanical few-body problems.* Berlin, Heidelberg: Springer-Verlag, 1998.

[17] K. Varga and Y. Suzuki, "Solution of few-body problems with the stochastic variational method. I. Central forces with zero orbital momentum," *Comp. Phys. Comm.*, vol. **106**, p. 157, 1997.

[18] J. R. Taylor, *Scattering Theory: The quantum theory of nonrelativistic collisions.* New York: Dover, 2006.

[19] M. L. Goldberger and K. M. Watson, *Collision theory*. New York: J. Wiley & Sons, 1964.

[20] K. A. Olive et al. (Particle Data Group), "Review of particle physics," *Chin. Phys. C*, vol. **38**, p. 090001, 2014. http://pdg.lbl.gov/xsect/contents.html.

[21] G. Audi and A. H. Wapstra, "The 1993 atomic mass evaluation. (I) Atomic mass table," *Nucl. Phys. A*, vol. **565**, p. 1, 1993.

[22] C. Samanta, P. R. Chowdhury, and D. N. Basu, "Generalized mass formula for non-strange and hyper nuclei with SU(6) symmetry breaking," *J. Phys. G*, vol. **32**, p. 363, 2006. arXiv:nucl-th/0504085.

[23] M. M. Block and R. N. Cahn, "High-energy $p\bar{p}$ and pp forward elastic scattering and total cross sections," *Rev. Mod. Phys.*, vol. **57**, p. 563, 1985.

[24] I. M. Dremin, "Elastic scattering of hadrons," *Physics-Uspekhi*, vol. **56**, p. 3, 2013. arXiv:1206.5474v4.

[25] C. Patrignani et al. (Particle Data Group), "2016 review of particle physics," *Chin. Phys. C*, vol. **40**, p. 100001, 2016. http://www-pdg.lbl.gov/2016/reviews/rpp2016-rev-cross-section-plots.pdf.

[26] J. Cudell, A. Lengyel, and E. Martynov, "The soft and hard Pomerons in hadron elastic scattering at small t," *Phys. Rev. D*, vol. **73**, p. 034008, 2006. arXiv:hep-ph/0511073; http://www.theo.phys.ulg.ac.be/~cudell/data/.